

▲ **Fig. 5:** Time variations of the apex height in dimensionless coordinates for a sessile drop measured during solvent loss at low humidity rate ($RH=30\%$; $\theta_0=40^\circ$; $R_0=3.1$ mm). After the primary buckling instability leading to an axisymmetric "peak", a secondary instability takes place and breaks the axisymmetry of the drop. Inset: image taken at 45° of such drop at the final stage of the drying process: radial wrinkles are clearly observable all around the peak formed by the first buckling instability (also in Figure 4b).

cascade of buckling events takes place, resulting in a complex pattern. At the final stage the top view of the drop is shown in the corresponding inset in Figure 1.

A sessile drop which dries would at first appear as a simple problem. However our experiments reveal that a combination of several processes take place during the drying process and that, depending on the experimental conditions, different morphologies can be observed at the drying end. These are strongly related to the different modes of the buckling instability which take place in an elastic shell. This leads to various shapes that exhibit axisymmetric or non-axisymmetric distortions. These phenomena are also related to a large variety of industrial applications including the formation of coatings. Such investigations may also help to solve a variety of problems in film, membrane or bio-interface mechanics.

References

This article is based on an original version published in the "Bulletin de la SFP" (French Physical Society), 140, p.4, Jul. 2003.

- [1] W. Flugge, Handbook of Engineering Mechanics; New York, McGraw-Hill (1962).
- [2] J. W. Hutchinson, J. Appl. Mech., 8, 49 (1967).
- [3] S. Timoshenko and J. M. Gere, in Theory of Elastic Stability; 2nd ed. New York, McGraw-Hill (1961).
- [4] F. Parisse and C. Allain, J. Phys. II, 6, 1111 (1996).
- [5] R. D. Deegan, O. Bakajin, T. F. Dupont, G. Huber, S. R. Nagel and T. Witten, Nature, 389, 827 (1997).
- [6] L. Pauchard and C. Allain Europhys. Lett., 62 (6), pp. 897-903 (2003); Y. Gorand, L. Pauchard, G. Callegari, J. P. Hulin, C. Allain Langmuir 20(12) pp. 5138-5140 (2004).
- [7] L. Pauchard, S. Rica Phil. Mag. B, 78 (1998).
- [8] J. M. Boffa, C. Allain and J. P. Hulin, Eur. Phys. J., AP 2 281 (1998).

Ternary and quaternary fission

Friedrich Gönnerwein¹, Manfred Mutterer² and Yuri Kopatch³

¹ Physikalisches Institut, Universität Tübingen, Germany

² Institut für Kernphysik, Technische Universität Darmstadt, Germany

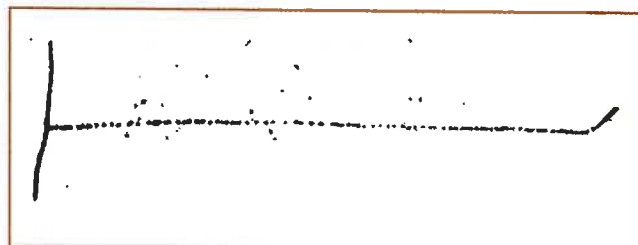
³ Frank Laboratory of Neutron Physics, JINR, Dubna, Russia

Nuclear fission has become known in the late thirties of the last century as a process where a heavy nucleus such as Uranium or Thorium decays into two fragments of about the same mass. The process was discovered while irradiating natural Uranium with thermal neutrons [1] and it soon became evident that among the U-isotopes it was ^{235}U to be held responsible for the reaction $^{235}\text{U}(n,f)$ observed. Shortly afterwards it was found that heavy nuclei such as ^{238}U may also undergo fission spontaneously [2].

Whether by spontaneous or induced fission, the mother nucleus disintegrates in the overwhelming fraction of cases just into two fragments. Fragmentation into three or more daughter nuclei of about equal mass has up to the present not been detected unambiguously. There is a full range of some 800 different fragment nuclei formed with as a rule the fragment being very neutron rich. A peculiarity of low energy fission is the asymmetry of the mass division: in the lighter actinides from Thorium to Einsteinium, the nuclei disintegrate asymmetrically in the sense that predominantly a heavier and a lighter fragment is produced. For example, in a fissioning nucleus such as ^{236}U , a typical ratio of heavy/light fragment mass numbers is 140/96.

Ternary fission

Sometimes instead of the standard "binary fission" a ternary process with three charged particles in the outgoing channel is observed, but with the third particle being very light compared to the fission fragments proper. This "ternary fission" process was discovered by several groups in the '40s of the last century. The technique was to soak photographic emulsions with Uranium salts and to irradiate the emulsion with thermal neutrons. Ionising particles leave tracks that after development of the emulsion may be visualised under a microscope. An example is provided in Figure 1 [3]. The two heavily ionising tracks starting at the vertex of the three-pronged event (in the figure upward and downward)



▲ **Fig. 1:** Ternary fission event observed in a photographic nuclear emulsion. From the vertex one fragment is moving upwards and the complementary fragment is moving downwards. The track to the right side is due to a long range α -particle. Reaction: $^{nat}\text{U}(n,f)$, from Ref. [3].

belong to the two main fission fragments. A third less ionising track is observed at roughly 90° to the axis formed by the fragments. From its ionisation density it was concluded that it must be an α -particle, i.e. the He-isotope ^4He . The first conjecture then was that it could be an α -particle from the radioactive decay of Uranium? But an α -particle from the radioactive decay of one of the isotopes of natural Uranium would have a kinetic energy not exceeding 5 MeV and its track length in emulsions should be comparable to the track length of the fission fragments. Therefore the “long range α ” seen in Figure 1 is definitely not due to radioactive decay. Instead, these α -particles must be formed in the process of fission.

The first question to be answered concerns the probability of ternary fission compared to binary fission. The systematic study of ternary fission with electronic detectors for fragments and light charged particles in coincidence revealed that the ratio t/b of the ternary to binary yield never exceeds a few tenths of a percent in low energy fission. Thus, ternary fission is indeed a very rare process. Another remarkable feature is that the yield ratio e.g. in thermal neutron induced fission stays close to $t/b \approx 2 \cdot 10^{-3}$ for reactions ranging from $^{229}\text{Th}(n_{\text{th}},f)$ up to $^{251}\text{Cf}(n_{\text{th}},f)$. In spontaneous fission the t/b ratios are slightly larger [4, 5]. In the following we will focus on these reactions where sources with large fission rates are available.

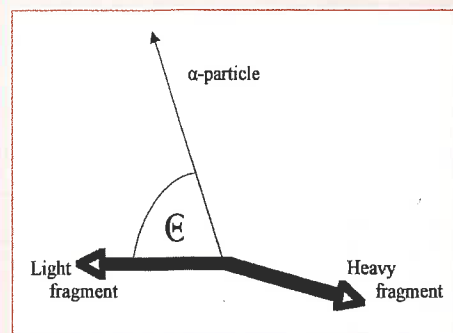
Where and when are ternary particles born ?

Next, one would like to know where and when the ternary particles are getting shape. Information on this question has come from the analysis of α -particle energies and of angular correlations between these particles and the fission fragments. A

Ternary fission

In standard nuclear fission the mother nucleus disintegrates in a binary decay into two fragments of comparable mass. Very rarely a light charged particle accompanies the main fragments. In most cases the third particle of ternary fission is an α -particle. The light particles are born together with the main fragments when the nucleus breaks apart at scission. From the angular distributions of these α -particles relative to the fragments it is concluded that they are formed in the neck region between the two separating fragments. The Coulomb force will then expel the light particle roughly at right angles to fragment motion as observed experimentally (cf. Figs. 1 and 2). By contrast, fission neutrons are evaporated from the fragments well after scission when the fragments have been fully accelerated by the Coulomb interaction.

In the drawing the lighter of the two main fragments is flying to the left. The emission angle Θ of the ternary α -particle is measured by convention relative to the direction of flight of the lighter fragment. Most α -particles are focused into a cone



at about right angles relative to fragment motion. Note that, due to momentum conservation, in ternary fission the strict collinearity of the two fragments is lost.

comprehensive overview of α -particle energies and emission angles is on display in Figure 2 for spontaneous fission of ^{252}Cf [5]. In the polar diagram each point corresponds to an α -particle event. The distance of the point from the centre characterises the kinetic energy and the polar angle Θ indicates the angle between the α -particle and the lighter of the two fragments. The lighter fragment flies in the figure at the polar angle $\Theta = 0^\circ$ to the left. Evidently the α -particles have a broad energy distribution with energies up to 30 MeV. As to the angular distributions, the majority of α -particles comes off roughly at right angles to the fission fragments. Both features could already be guessed from the observation of single events such as that shown in Figure 1. It is obvious from Figure 2 that the angular distribution is not perfectly symmetric relative to the polar angle 90° . Instead, the distribution is shifted towards polar angles smaller than 90° , i.e. in direction of the lighter fragment.

Intuitively the characteristics of the angular distributions point to an emission of α -particles from a region between the two nascent fragments. This can be seen from the following arguments. Since upon scission of a dividing nucleus a short lived neck joining the two fragments is formed, it is tempting to conjecture that α -particles are formed while the neck is rupturing. Ternary particles are in this view remnants of the neck. Stated in other words, binary fission should correspond to a single rupture of the neck filament, while in ternary fission the neck is cut at two places before the stubs of the neck can recede and be absorbed by the fragments. Thus a third particle is set free [6]. The combined Coulomb forces from the two heavier fragments acting on the light charged particle will then accelerate this particle and push it out of the neck region at roughly right angles to the fission axis, or more precisely, as observed in experiment (cf. Fig. 2), at an angle slightly shifted towards the light fragment. This is attributed to the fact that the push exerted by the heavier fragment carrying a higher nuclear charge is larger than the one due to the light fragment. The above simple picture has been substantiated by trajectory calculations of several authors where essentially the Coulomb forces between the three bodies come into play

A more delicate question is at what stage of the fission process is the decision taken to emit an α -particle. Is the formation of an α -particle already settled at a very early stage of fission when the fission-prone nucleus just starts to deform? Or does the α -particle come into view at the saddle point of deformation, i.e. at the fission barrier, when the nucleus is bound to continue on its way to scission? Or does the α -particle only take shape at the very last stage of scission? A key to answer this question has been found while investigating the angular distributions of fission fragments and comparing the anisotropies observed in binary and ternary fission. According to theory the angular distributions of fragments are determined by the wave functions describing the transition states of the saddle point. The remarkable result for all reactions analysed is that the angular distributions of fission fragments are identical in binary and ternary fission. Hence, at the saddle point, there is no trace whatsoever of ternary particles. The light particles must be born in the last stage of the process near or right at scission during neck rupture [7]. There are good reasons to believe that neck rupture is a process quite similar to the instabilities of a filament of water analysed by Lord Rayleigh at the end of the nineteenth century. Fluctuations in the microscopic motion of nucleons in the neck should introduce an element of randomness and both the location of the cut and the number of cuts are expected to exhibit fluctuations that lead either to binary or ternary fission.

Ternary particles other than α -particles

So far only α -particles were addressed as the light ternary particles. Though α -particles contribute $\sim 90\%$ and hence the lions share to the total ternary yield, there are many other light ions which become observable as ternary particles [4,5]. The most important ones to be mentioned are the hydrogen isotopes, viz. protons, deuterons and tritons. They carry $\sim 1\%$, $\sim 0.5\%$ and $\sim 6\%$ of the total yield, respectively, the neutron-rich triton being the most abundant hydrogen isotope amongst the ternary particles. Neutron-rich isotopes also dominate the yield of other elements. For example, the isotope ^3He has so far completely escaped detection. By contrast, in the heavier elements the neutron-rich isotopes, ^6He , ^8He , ^9Li , ^{10}Be , ^{13}B and ^{14}C for example, have sizable yields [5].

The favoured production of neutron-rich isotopes has led to the conjecture that possibly neutrons could also be ejected at scission. However, there is only indirect evidence for their existence. In experiments aiming at a direct detection no scission neutrons were seen.

The heaviest ternary particles observed

One may wonder which are the heaviest nuclei to be detected and identified as ternary particles. Experiments are difficult due to the fact that besides ternary fission being a rare process, the yield for nuclei heavier than ^4He is only some 3% of the total ternary yield. In the search for the heaviest ternary particles the electromagnetic mass separator "Lohengrin" installed at the High Flux Reactor of the Laue-Langevin Institut in Grenoble/France has proven to be an ideally suited instrument. The ion source of Lohengrin is just a thin layer of fissile material irradiated by neutrons from the reactor. Any charged ions such as fission fragments or charged ternary particles emitted by the source and intercepted by the spectrometer will be analysed according to their mass and energy. With a standard ΔE - E_{rest} detector installed in the focal plane of the spectrometer the nuclear charges of the ions are also assessed. Systematic studies have been conducted for thermal neutron-induced reactions on target nuclei ranging from ^{233}U up to ^{249}Cf . Results for the two reactions $^{235}\text{U}(n_{\text{th}},f)$ and $^{249}\text{Cf}(n_{\text{th}},f)$ are on display in Figure 3 [8]. The yields of ternary particles per 100 fission reactions are given in the left part of the figure. For the ^{235}U target the heaviest ternary particle to be observed at the limit of detection of the instrument was ^{22}O , while for the ^{249}Cf target the heaviest isotopes were ^{37}Si and ^{37}S . Yields down to $3 \cdot 10^{-9}$ per fission event could be measured. The yield curves are not levelling off and, hence, heavier ternary particles with still lower yields are expected to be produced.

One may ask why at the same level of yields in Figure 3 the masses of ternary particles increase with the mass of the mother nucleus when comparing the two reactions $^{235}\text{U}(n_{\text{th}},f)$ and $^{249}\text{Cf}(n_{\text{th}},f)$. An answer may be found by inspecting the fragment mass distributions. These are shown in the right part of Figure 3. The binary fragment mass distributions conspicuously exhibit the asymmetric split of the mother nucleus, leading to a heavy and a light fragment group. It is worthwhile to point out that the fragment yields for the two reactions under study coincide at mass numbers around $A \approx 132$ in the heavy mass group and around $A \approx 76$ in the light mass group. The mass $A = 132$ is singled out due to the extra-stability of the ^{132}Sn nucleus with a magic $Z = 50$ proton cluster and a magic $N = 82$ neutron cluster. The shell-stabilisation of ^{132}Sn (and some neighbouring nuclei) is, in fact, understood to be one of the roots for the preference of asymmetric mass splits in the actinides. Similarly, in the light mass group one may anticipate the influence of the magic proton cluster

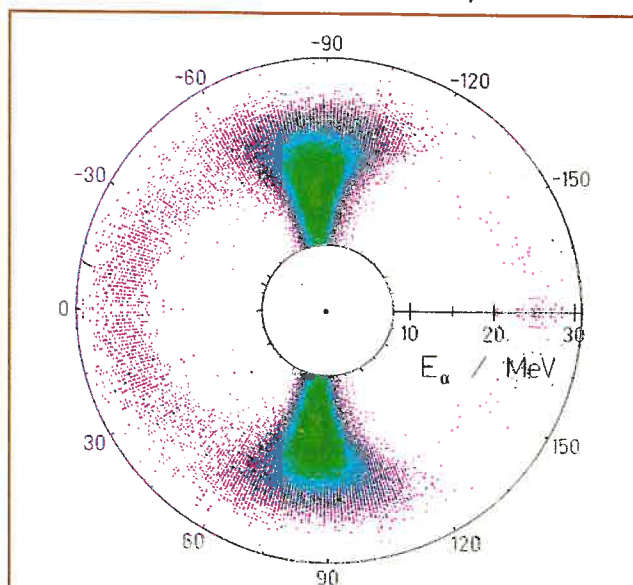
$Z = 28$ (Ni) and the magic neutron cluster $N = 50$. Though the doubly magic nucleus ^{78}Ni could not be detected in low energy fission, nevertheless, the cooperation of the two magic clusters is thought to be responsible for the enhancement of yields in the mass number window $A = 70$ to $A = 80$, a phenomenon having been called "super-asymmetric" fission.

What can now be learned from asymmetric and super-asymmetric fission for the yields in ternary fission? Again a simple picture might be helpful. Let us assume that for the reactions under study in the heavy fragment there is an $A = 132$ core and in the light fragment an, say, $A = 76$ core which both strongly resist being broken up. This would then leave for the number of neck nucleons in fission of $^{236}\text{U}^*$: $[236 - (132+76)] = 28$ nucleons and in fission of $^{250}\text{Cf}^*$: $[250 - (132 + 76)] = 42$ nucleons. The increase in available number of neck nucleons in Cf compared to U therefore explains the increase in yield of heavy ternary particles for increasing mass numbers of the mother nucleus.

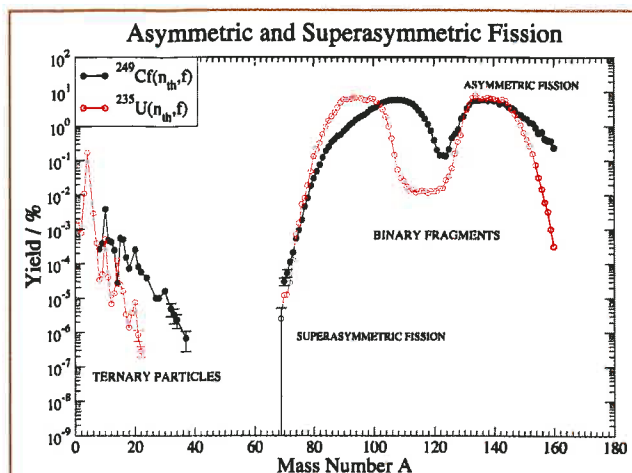
As seen in the figure there is still a gap in mass number between the heaviest ternary particles and the lightest fission fragments. In the cluster picture outlined for the scission configurations this is indeed not surprising. However, the probability of breaking up the cluster cores, although small, is strictly speaking not zero. Therefore, one should expect non-zero yields also in the gap region of masses in Figure 3, albeit at yield levels that are presently inaccessible. Interestingly, as the excitation energy of the fissioning nucleus is raised, the gap is rapidly filled and the ternary and binary yield distributions are smoothly joined.

Mass distributions of fragments in ternary fission

We stress once more that the mass distributions on display in Figure 3 are for fragments from binary fission. In ternary fission these fragment mass distributions will certainly be different. The



▲ Fig. 2: Scatter plot of ternary α -particle emission from $^{252}\text{Cf}(sf)$. In the polar diagram the fissioning nucleus is located at the centre with the light fragment moving to the left ($\Theta = 0^\circ$) and the heavy fragment to the right ($\Theta \approx 180^\circ$). Each point in the plot corresponds to an α -particle from ternary fission. Energies of the α -particles are represented as radii measured from the centre. Their angles of emission relative to light fragment momentum are given as the polar angles Θ of the radius vector, from ref. [5].



▲ **Fig. 3:** On the right side are depicted the mass yields from binary fission of $^{249}\text{Cf}(n_{th},f)$ and $^{235}\text{U}(n_{th},f)$ as black and red circles, respectively. On the left side are shown the mass yields of ternary particles from the same two reactions, from ref. [7].

differences will be the more pronounced the heavier the ternary particles are, since more and more nucleons are missing for the formation of fragments. Results for the spontaneous fission reaction $^{252}\text{Cf}(sf)$ are presented in the following. In experiment, besides the two main fragments, the ternary particle energies, masses and charges were measured in coincidence [8, 9]. The fragment mass distributions in ternary fission are shown in Figure 4 for ^4He and for Be isotopes as the ternary particles. Data points are for fragments from ternary fission while the dashed red lines trace the distributions from binary fission for comparison. The binary and ternary yields have been normalised to the same number of events. It must be pointed out, however, that for experimental reasons the ternary mass distributions pertain to ternary particle energies in excess of 8 MeV and 26 MeV for ^4He and the Be-isotopes, respectively. It is obvious from the figure that in going from binary to ternary fission the mass distributions are not displaced as a whole but are getting narrower the heavier the ternary particle is. Most remarkably the mass number of the lightest fragment in both the heavy and the light mass group appears to stay constant while the heaviest fragment in both groups is shifted downward to smaller masses. It should be noted that the lightest fragment in the light group is complementary to the heaviest fragment in the heavy group (asymmetric fission) and vice versa for the lightest fragment in the heavy group and the heaviest fragment in the light group (near symmetric fission). In order to compensate for the loss in nucleon numbers going into the ternary particles, at fixed mass numbers of the lightest fragments the fragment mass distributions have to become narrower the heavier the ternary particle is.

It is tempting to attribute the characteristic changes in the mass distributions once more to the cluster structure of fragments. It again appears that both in the light and the heavy fragment the shell-stabilised clusters discussed in connection with Figure 3 are resistant to break-up. These clusters fix the locations of the foothills to the left of the two humps for both, light and heavy fragments. In the heavy group the stabilisation of mass numbers around mass $A = 132$, with the key nucleus being ^{132}Sn , is readily recognised. For the light group we have to recall that the stabilising effect for mass numbers around $A = 76$ sets in at very low fission yields, in fact too low to become detectable in the rare ternary decay (cf. Fig. 3).

Neutron emission in ternary fission

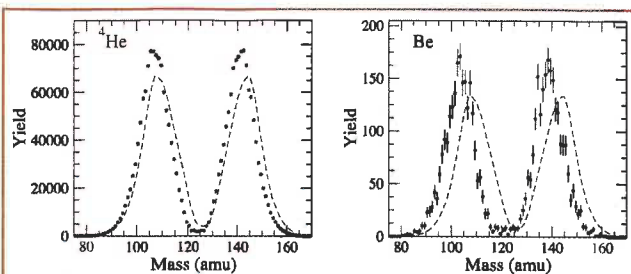
The study of neutron emission from fragments in ternary fission gives additional support to the role played by nuclear shell structure in the process. In the experiment on $^{252}\text{Cf}(sf)$ already quoted [9], the chamber where the charged particles were registered was placed at the centre of the Heidelberg crystal ball [10]. The ball with its 162 NaI(Tl) crystals is primarily a γ -detector but also allows neutrons to be detected. Thus neutron emission from fragments in ternary reactions could be studied for different types of ternary particles. A sample of results is displayed in Figure 5 [9] where, for the same ternary reactions with ^4He and Be-isotopes accompanying fission shown in Figure 4, the neutron multiplicity numbers $\langle\nu(A)\rangle$ as a function of fragment mass A are plotted. Data from ternary fission are shown as black circles with error bars. The neutron multiplicities from binary fission are sketched for comparison as dashed red curves.

For discussion it should be noted that neutrons (and to a lesser extent also γ -quanta) carry away the excitation energy of fragments. At scission, however, the main part of the excitation energy of the eventual fragments is still tied up as deformation energy. After scission the deformation will relax and the energy liberated will be found back in the intrinsic energy of the fragments. The neutron multiplicity thus carries information on the deformation of fragments at scission. With this correspondence in mind the sawtooth-like shape of the neutron multiplicity $\langle\nu(A)\rangle$ in Figure 5 is an intriguing feature of nuclear fission. Striking to eye is the virtual disappearance of neutron multiplicity near mass $A = 132$. A similar vanishing multiplicity is also observed for masses near $A = 80$ which is, however, not shown in Figure 5. This says that the cluster-like fragments, having been repeatedly referred to as being extra-stable, are also extra-stiff and survive the elongation process of fission without being appreciably deformed themselves. By contrast, the complementary fragments emitting many neutrons were strongly deformed at scission. In fact, in binary fission of $^{252}\text{Cf}(sf)$ the peak in the neutron distribution is found at mass $A = 120$, *i.e.* exactly complementary to the heavy cluster with mass $A = 132$.

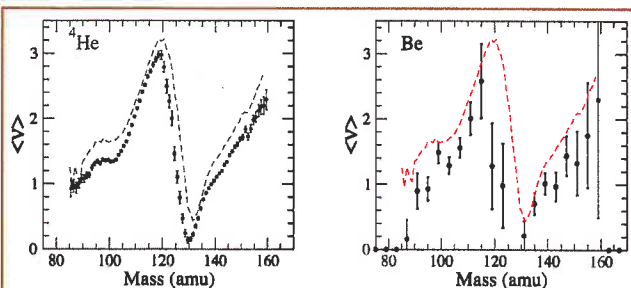
As is evident from the figure, the neutron multiplicities in ternary fission are generally lower than in binary fission. For example, in $^{252}\text{Cf}(sf)$ the multiplicity $\langle\langle\nu\rangle\rangle$ averaged over all mass splits is 3.77 in binary and 3.07 in α -accompanied fission [11]. In ternary fission with Be as the ternary particle the neutron multiplicity drops even lower to about 2.6 [9]. The decrease in neutron number implies that some of the fragment excitation energy, which at scission is stored as deformation, is consumed by ternary particle emission. A still more detailed insight is obtained from inspecting the mass-dependent neutron multiplicity $\langle\nu(A)\rangle$. In particular Figure 5 shows that for Be accompanied fission the multiplicity peak observed in binary fission at $A = 120$ has shifted downward towards smaller mass numbers of the light fragment. Since among the ternary Be yields the isotope ^{10}Be by far dominates the yield, in fission accompanied by the emission of Be-isotopes the light fragment mass $A = 110$ is complementary to the heavy fragment mass $A = 132$. As seen in Figure 5, in experiment the multiplicity peak in the light fragment comes indeed close to $A \approx 110$. This appears to indicate that also in ternary fission a maximum of deformation is accumulated in fragments complementary to the cluster fragments.

Unstable ternary particles and quaternary fission

Although the main lines of ternary fission have now been traced there are many more interesting facets of this process to be disclosed.



▲ **Fig. 4:** Fragment mass distributions in ternary fission of $^{252}\text{Cf}(sf)$ with ^4He and Be as the light charged particles (black points with error bars in the left and right panel, respectively). Yields are given as the number of events measured. Binary mass distributions are shown for comparison as red dashed curves. For each reaction the binary distributions are normalised to the total number of counts in the ternary distribution, from ref. [8].



▲ **Fig. 5:** Neutron multiplicities as a function of fragment mass in ternary fission of $^{252}\text{Cf}(sf)$ with ^4He and Be as the light charged particles (black points with error bars in the left and right panel, respectively). Neutron multiplicity data from the corresponding binary fission reaction are given as dashed red curves, from ref. [8].

In particular the measurement of particle-unstable ternary particles has been of importance because in some cases the decay products may contribute to the yields of lighter ternary particles. Prominent examples of unstable ternary particles are the He-isotopes ^5He and ^7He . They decay by neutron emission with lifetimes of $1.1 \cdot 10^{-21}\text{s}$ and $4.1 \cdot 10^{-21}\text{s}$, respectively, and therefore well before being intercepted in charged particle detectors. Their yields in $^{252}\text{Cf}(sf)$ could be determined in recent experiments by exploring the angular correlations between neutrons and the ternary particles [12]. A remarkable result is the large percentage of ^4He and ^6He observed in charged particle detectors which in reality are the remnants of ^5He and ^7He following n-decay. The yield ratios $^5\text{He} / ^4\text{He}$ and $^7\text{He} / ^6\text{He}$ are both equal to 0.21(5). This means that only about 83 percent of the α -particles measured are in reality primary α -particles while about 17% have originally been created as ^5He nuclei. Behind ^4He , the second most important ternary particle is the He-isotope ^5He , and not the H-isotope ^3H as was held to be true in the past.

Besides ternary isotopes being unstable to n-decay, charged particle decay has also to be taken into account. A prominent example is ^8Be with a lifetime of $6.7 \cdot 10^{-17}\text{s}$ for the ground-state decay $^8\text{Be} \rightarrow (\alpha + \alpha)$. This decay is intriguing because the $(\alpha + \alpha)$ events observed could also be due to a simultaneous emission of two light charged particles in a single fission decay. In contrast to ternary fission with only one charged light particle the above processes are called quaternary fission. The way to disentangle true quaternary $(\alpha + \alpha)$ events from the sequential

decay of ^8Be into $(\alpha + \alpha)$ is by analysing the angular correlations between the two α -particles. Studies of quaternary fission have been performed for spontaneous and thermal neutron-induced reactions. For the $^{252}\text{Cf}(sf)$ reaction it is found that the yield for simultaneous $(\alpha + \alpha)$ emission is about 10^{-6} per fission while the production of ^8Be is about three times more probable. In the reactions $U(n_{th},f)$ with either the ^{233}U or ^{235}U isotope as target these yields are down by roughly an order of magnitude [13].

Gamma emission in ternary fission

Let us close the present survey of ternary fission phenomena with a remark on γ -emission in fission. Gamma-rays carry away the fragment excitation energy left behind after neutron evaporation. In addition, they bear information on the angular momentum the fragments acquire near scission. Remarkably, it is found that the spins are oriented at right angles to the fission axis. Models are explaining this orientation of fragment spins by a butterfly-like oscillation of the two deformed fragments facing each other at scission but still sticking together [14]. These rotary oscillations impart spin to the fragments which is indeed pointing at right angles to the fission axis. Spin orientation leads to anisotropic γ -emission relative to the fission axis. As regards ternary fission one should expect that in a strongly excited butterfly mode the ternary particles are released in the direction of motion of the two fragment tips in the rotary oscillation. However, no indication of correlated gamma-ternary particle emission has been found in experiment [15]. This particular result adds to the more general difficulties in understanding the generation of angular momentum in fission fragments.

Finally, let us stress that beyond this specific problem of angular momentum, ternary fission continues to be not merely a curious peripheral-aspect of fission but, as shown in the present survey, is a precious source of information on the complex, and in many respects still puzzling, fission process as a whole.

References

- [1] O. Hahn and F. Strassmann, *Naturwissenschaften* 27, 89 (1939)
- [2] K. A. Petrzhak and G. N. Flerov, *J. Phys.*, USSR 3, 275 (1940)
- [3] Tsieng San-Tsiang et al., *Phys. Rev.* 71, 382 (1947)
- [4] C. Wagemans in *The Nuclear Fission Process* (CRC Press, ed. C. Wagemans, 1991),
- [5] M. Mutterer and J. P. Theobald in *Nuclear Decay Modes* (IOP Press, ed. D. N. Poenaru, 1996)
- [6] V. A. Rubchenya, *Sov. J. Nucl. Phys.* 35, 334 (1982)
- [7] F. Gönnerwein, *Proc. Conf. Nuclear Data for Science and Technology*, Santa Fe, USA, 2004, to be published
- [8] F. Gönnerwein, *Nucl. Phys. A* 734, 213 (2004)
- [9] M. Mutterer et al., to be published
- [10] P. Singer et al., *Zeitschr. f. Phys. A* 359 41 (1997) and PHD thesis, TU Darmstadt 1997
- [11] G. K. Mehta, et al., *Phys. Rev. C* 7, 373 (1973)
- [12] Yu. N. Kopatch et al., *Phys. Rev. C* 65, 044614 (2002)
- [13] P. Jesinger et al., to be published
- [14] J. O. Rasmussen et al., *Nucl. Phys. A* 136 465 (1969)
- [15] Yu. N. Kopatch et al., *Phys. Rev. Lett.* 82, 303 (1999)